© Universiti Tun Hussein Onn Malaysia Publisher's Office

IJIE

Journal homepage: http://penerbit.uthm.edu.my/ojs/index.php/ijie
ISSN : 2229-838X e-ISSN : 2600-7916

The International Journal of Integrated Engineering

Performances of Six-leg DSTATCOM Topology under Various SRF Algorithms

Pradeep Kumar[1]

[1]EEED, NIT Sikkim, Ravangala 737139 INDIA

*Correspoding Author

DOI: https://doi.org/10.30880/ijie.2020.12.08.016
Received 13 September 2019; Accepted 20 January 2020; Available online 31 August 2020

Abstract: Six-leg DSTATCOM can be employed for improving the superiority of power in a distribution system. DSTATCOM is the most valuable current harmonic reduction device because of its excellent compliance in active situations. The DSTATCOM has a shunt voltage source inverter (VSI) attached to the common coupling point of power system via the interfacing inductor. In its control methodologies, the various SRF methods such as Conventional SRF, DCC based SRF and ICC based SRF have been adopted due to its easy execution aspects. These methodologies create balanced and sinusoidal supply current. Improving the power factor near unity on common coupling point and mitigate harmonics in the supply current will be the key results of this work. A 3-phase 4-wire power system with rectified RC/RL load has been taken for the detailed simulation study. The performances of DSTATCOM topology have been compared under conventional SRF, DCC based SRF and ICC based SRF control strategies in terms of power quality improvement.

Keywords: Distribution static compensator (DSTATCOM), Synchronous reference frame (SRF), Indirect current controlled (ICC), Direct current controlled (DCC), Power quality (PQ).

1. Introduction

Due to the non-stop increases of power electronic based appliances in the commercial, agricultural, industrial and domestic field, the superiority of power in a distribution network is degrading too much [1,2]. In this serious circumstance, the power engineers and researchers have a major job to distribute high superiority power to the modern humanity. Now several power quality problems i.e. unbalanced three- phase load voltage, less power factor, extreme current in the neutral wire and peak reactive power which are elevated in a 3-phase 4-wire (3P4W) distribution network[3-9]. The alleviation of the above power quality difficulties is accounted in the literature [2,4,7,9,10]. Moreover, various custom power devices (CPDs) are tackled in [7,10] to boost the superiority of power in a 3P4W power system. DSTATCOM is one of the custom power devices which efficiently control power transfer in the power system. The STATCOM employed in the distribution system is known as DSTATCOM. The basic of STATCOM is to regulate flow of power and recover transient stability of power system. A vast investigation of different DSTATCOM topologies has been discussed in [11-15]. The performance of a DSTATCOM in power quality alleviation is definitely based on rapidness and perfectness of its control approaches. Various studies on control approaches have been depicted in the text such as Synchronous Reference Frame (SRF) [16-19], Instantaneous Power Theory [20,21], wavelet technique [22], Neural Network (NN) [23, 24] etc. The SRF control approach demonstrates major benefits with respect to other control approaches such as effortless design, fast speed and fewer computations, which provides much efficient for its practical implementation. This work elaborates on performance analysis of DSTATCOM topology under conventional SRF, DCC based SRF and ICC based SRF control strategies in terms of power quality improvement.

*Corresponding author: pradeep@nitsikkim.ac.in

Organization of this paper is in the following manner. This paper has been started with the introduction in section 1, section 2 briefly presents the operational theory of DSTATCOM. Section 3 gives information about SRF control signals such as conventional, DCC based and ICC based SRF control techniques. Section 4 indicates the detailed analysis of MATLAB/simulation outcomes for the DSTATCOM system and last section 5 concludes this research work.

2. Operational Theory of DSTATCOM

The key component of the DSTATCOM structure is the voltage source inverter (VSI) where totally managed semiconductor appliances are employed. The fundamental theory of a DSTATCOM is the production of a regulated AC voltage supply from a VSI attached with a DC capacitor. The AC voltage supply comes out at both ends of transformer leakage reactance. The flow of real and imaginary power among the distribution system and the DSTATCOM is due to the potential diversity across this reactance. All necessary voltages and currents are assessed and are supplied to the controller. The controller generates output which is a set of switching signals for the inverter consequently. Practical configurations of DSTATCOM and its control schemes are elaborated in [7].

The key aspects of the DSTATCOM are the following [25, 26]:

(i) Capability to act different tasks at the same time;

(ii) Capability to track fast load alterations;

(iii) Under varying load situation, it is simple to apply in a distribution network.

Fig.1 represents a pictorial view of Distribution static compensator (DSTATCOM), shunted with the load and three phase supply at PCC. The load is unbalanced R-L and diode with RC/RL type. This is the main causes of harmonics [27,28] in a distribution network. The VSI is coupled to the distribution network via coupling transformer. The PWM pattern is used to switch on and off the semiconductor switches of the VSI [29]. The controller block represents conventional SRF/DCC based SRF/ ICC based SRF[30].

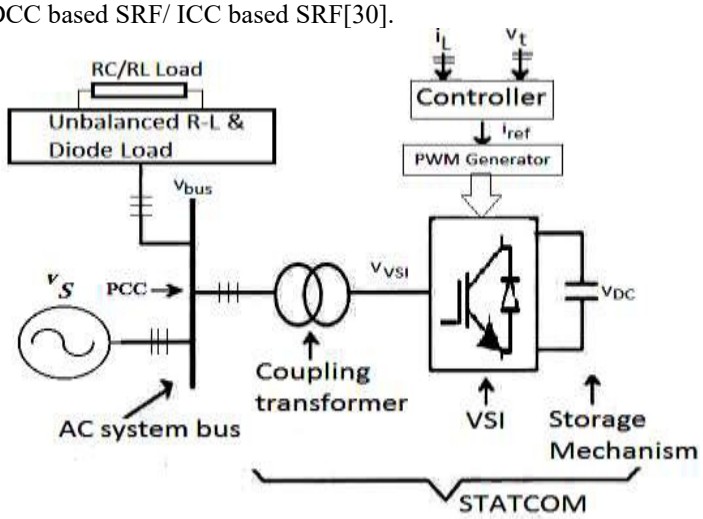

Fig. 1 - Pictorial view of DSTATCOM

Selection of different DSTATCOM components are as follows:

2.1 DC bus voltage:

The voltage across capacitor of DC-side three phase VSI is V_{dc} [19]

$$V_{dc} = 2\sqrt{2}V_{LL} / (\sqrt{3}m) \quad (1)$$

The modulation depth m is assumed as 1 and V_{LL} is the voltage between two phases. Hence calculated value of V_{dc} is 653.20V for 400Vof V_{LL} and is assumed as 700V.

2.2 DC capacitor:

For energy conservation theory [19],

$$(1/2)C_{dc}[V_{dc}^2 - V_{dc1}^2] = 3V(aI)t \quad (2)$$

Assuming, 2 % voltage ripple in the dc bus, the lower voltage point of dc bus, V_{dc1}= 686V, and V_{dc}= 700 V, V=230.94V, I= 195.7A, t= 235 μ s, a= 1.2, the computed value of C_{dc} is 3940.93μ F and hence C_{dc} is considered as 4000μF.

2.3 Filtering inductor:

Assuming, switching frequency (f_s) = 10 kHz, m=1, V_{dc} = 700V, a=1.2, the L_f is computed as [19],

$$L_f = mVdc / 4af_{s\,cr(p-p)} \quad (3)$$

For, 2 % ripple in the inductor current, the current ripple $i_{cr(p-p)}$ = 0.02*195.7*240/200= 4.70A, the computed value of L_f is 3.10 mH and hence L_f is considered as 3.0 mH.

3. Control Strategies

Control Strategies are employed to generate reference current by the reference current extraction method and this method is categorized into time-domain and frequency-domain. The advantage of time-domain method has rapid response compared to frequency-domain [31-33]. The time domain based synchronous reference frame theory is employed for extorting the reference current from the non-linear load current. The main feature of SRF theory is the straightforwardness of the computations, which contains merely arithmetical computation [34-36]. There are three categories of SRF control techniques; (i) conventional-SRF (ii) DCC based SRF and (iii) ICC based SRF.

3.1 Conventional-SRF

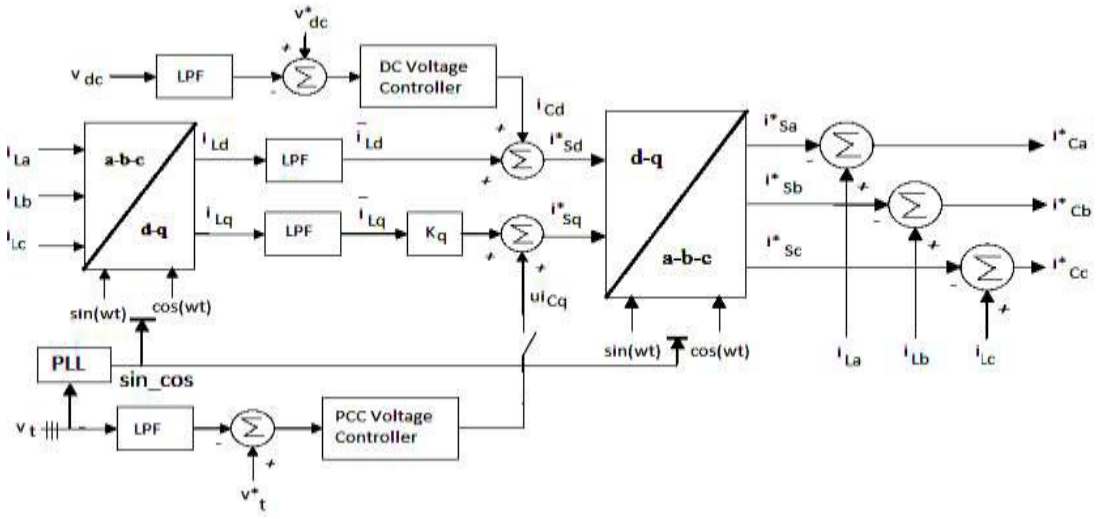

Fig. 2 - Conventional SRF

In Fig. 2, three phase reference compensator current is obtained from the three phase load current and PCC voltage. Three phase PLL has been employed to generate unit vector component for the a-b-c to d-q transformation and d-q to a-b-c transformation. The a-b-c to d-q transformation has been achieved by the following formulation:

$$\begin{bmatrix} i_{Ld} \\ i_{Lq} \end{bmatrix} = \frac{2}{3}\begin{Bmatrix} \cos\omega t & \cos\left(\omega t - \frac{2\pi}{3}\right) & \cos\left(\omega t + \frac{2\pi}{3}\right) \\ \sin\omega t & \sin\left(\omega t - \frac{2\pi}{3}\right) & \sin\left(\omega t + \frac{2\pi}{3}\right) \end{Bmatrix}\begin{bmatrix} i_{La} \\ i_{Lb} \\ i_{Lc} \end{bmatrix} \quad (4)$$

$$\begin{bmatrix} \overline{i_{Ld}} \\ \overline{i_{Lq}} \end{bmatrix} = G(s)\begin{bmatrix} i_{Ld} \\ i_{Lq} \end{bmatrix} \quad (5)$$

$\overline{i_{Ld}}$, $\overline{i_{Lq}}$ = Average load current in d-q frame

G(s) = Transfer function of LPF

For the power factor regulation, K_q is evaluated as

$$K_q = \frac{Q_s^*}{Q_L} \quad (6)$$

For power factor correction, $\cos\varphi = 1$, so $\varphi = 0$

$Q_S^* = VI\sin\varphi = 0$ hence $K_q = 0$

The reference supply currents (in d-q phase) are

$$i_{Sd}^* = \overline{i_{Ld}} + i_{Cd} \quad i_{Sq}^* = K_q\overline{i_{Lq}} + ui_{Cq} \quad (7)$$

The d-q to a-b-c conversion has been achieved by the following computation:

$$\begin{bmatrix} i^*_{sa} \\ i^*_{sb} \\ i^*_{sc} \end{bmatrix} = \frac{2}{3} \begin{Bmatrix} \cos\omega t & \sin\omega t \\ \cos\left(\omega t - \frac{2\pi}{3}\right) & \sin\left(\omega t - \frac{2\pi}{3}\right) \\ \cos\left(\omega t + \frac{2\pi}{3}\right) & \sin\left(\omega t + \frac{2\pi}{3}\right) \end{Bmatrix} \begin{bmatrix} i^*_{sd} \\ i^*_{sq} \end{bmatrix} \tag{8}$$

The reference three phase injecting currents are

$$i^*_{Ca} = i_{La} - i^*_{Sa}, \quad i^*_{Cb} = i_{Lb} - i^*_{Sb}, \quad i^*_{Cc} = i_{Lc} - i^*_{Sc} \tag{9}$$

3.2 DCC based SRF

The Complete process about reference current extraction of DCC based SRF is shown in Fig. 3. The input parameters for the DCC based SRF are three phase load current, three phase PCC voltage and DC bus current.

$$\begin{bmatrix} i_{Ld} \\ i_{Lq} \\ i_{L0} \end{bmatrix} = \frac{2}{3} \begin{bmatrix} \sin(\omega t) & \sin(\omega t - \frac{2\pi}{3}) & \sin(\omega t + \frac{2\pi}{3}) \\ \cos(\omega t) & \cos(\omega t - \frac{2\pi}{3}) & \cos(\omega t + \frac{2\pi}{3}) \\ \frac{1}{2} & \frac{1}{2} & \frac{1}{2} \end{bmatrix} \begin{bmatrix} i_{La} \\ i_{Lb} \\ i_{Lc} \end{bmatrix} \tag{10}$$

Where ωt depicts the phase shift of the d-q component. The real i_{Ld} and i_{Lq} components are

$$\begin{bmatrix} i_{Ld} \\ i_{Lq} \end{bmatrix} = \begin{bmatrix} i_{Ld(dc)} + i_{Ld(ac)} \\ i_{Lq(dc)} + i_{Lq(ac)} \end{bmatrix} \tag{11}$$

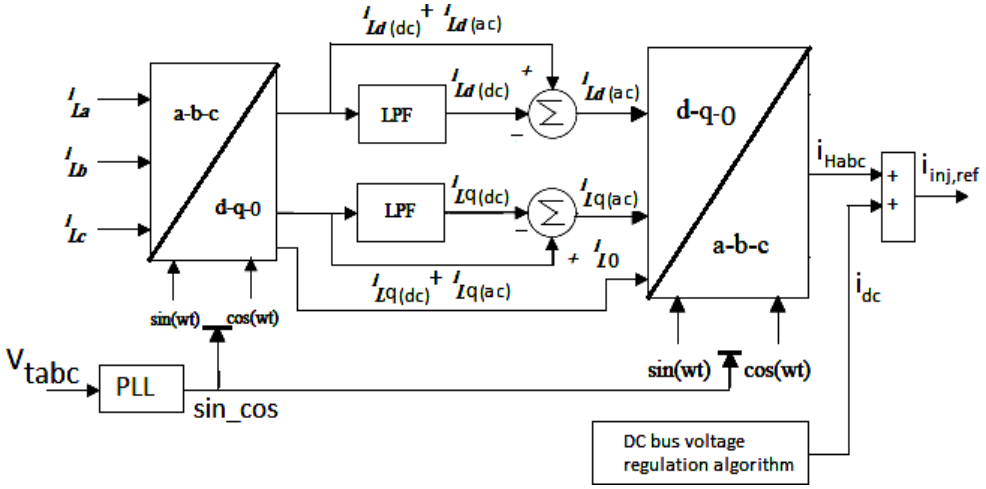

Fig. 3- DCC based SRF

where $i_{Ld\,(dc)}$ and $i_{Ld\,(ac)}$ indicate the dc and ac parts of the load current correspond to d- component and $i_{Lq(dc)}$ and $i_{Lq(ac)}$ depicts dc and ac parts of the load current correspond to q- component respectively.

For the reason of harmonics elimination, the $i_{Ld\,(ac)}$ and $i_{Lq(ac)}$ components are needed for reference current production. These ac components are achieved by subtracting the dc component from the real load current in the d-q frame. This formulation can be mentioned as below:

$$\begin{bmatrix} i_{Ld(ac)} \\ i_{Lq(ac)} \end{bmatrix} = \begin{bmatrix} i_{Ld} - i_{Ld(dc)} \\ i_{Lq} - i_{Lq(dc)} \end{bmatrix} \tag{12}$$

Once the ac components $i_{Ld\,(ac)}$ and $i_{Lq(ac)}$ are extorted, the Inverse Park-conversion is carried out to convert the ac components reverse into real three-phase harmonic current i_{Habc}, which in-turn, employed to develop the needed reference injection current.

$$\begin{bmatrix} i_{Ha} \\ i_{Hb} \\ i_{Hc} \end{bmatrix} = \begin{bmatrix} \sin(\omega t) & \cos(\omega t) & 1 \\ \sin(\omega t - \frac{2\pi}{3}) & \cos(\omega t - \frac{2\pi}{3}) & 1 \\ \sin(\omega t + \frac{2\pi}{3}) & \cos(\omega t + \frac{2\pi}{3}) & 1 \end{bmatrix} \begin{bmatrix} i_{Ld(ac)} \\ i_{Lq(ac)} \\ i_{L0} \end{bmatrix} \tag{13}$$

The reference injection current is given as:

$$i_{injref} = i_{Habc} + i_{dc} \tag{14}$$

Where i_{dc} indicates the instantaneous DC current, which is obtained from the DC-side of VSI.

3.3 ICC based SRF

Although the conventional SRF and DCC based SRF control schemes have been observed as a simple and efficient control scheme in power quality improvement, these control schemes still acquire weaknesses and needless aspects which might affect the power quality improvement performance. Hence, further modifications are employed, which results in the creation of the ICC based SRF control approach as shown in Fig. 4.

The two main enhancements of ICC based SRF control approach is underlined as below:

(i) The complexity of control approach is reduced with the elimination of cosine (q frame) and zero-sequence (0 frame) constituents.

(ii) In its place of a non-sinusoidal harmonic current, sinusoidal current is produced in the form of output.

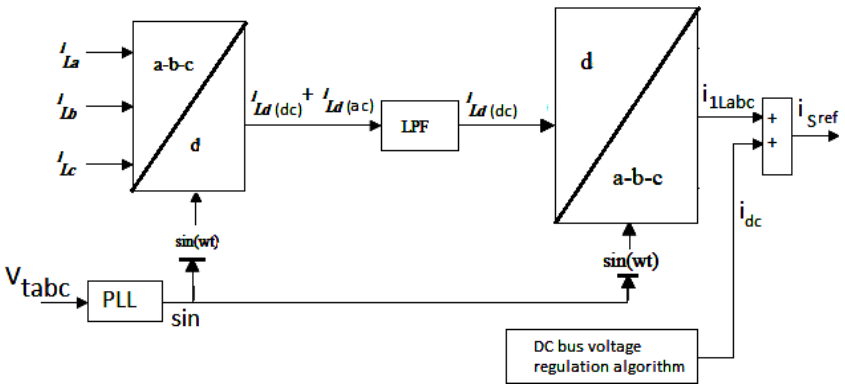

Fig. 4 - ICC based SRF

After eliminating the cosine constituent and zero-sequence constituent in the computation, the Park-transformation is modified as:

$$[i_{Ld}] = \frac{2}{3}\begin{bmatrix} \sin(\omega t) & \sin(\omega t - \frac{2\pi}{3}) & \sin(\omega t + \frac{2\pi}{3}) \end{bmatrix} \begin{bmatrix} i_{La} \\ i_{Lb} \\ i_{Lc} \end{bmatrix} \tag{15}$$

An LPF has been employed to acquire dc quantities from the i_{Ld} i.e. $i_{Ld\,(dc)}$. In this way, non-dc quantities are eliminated. The inverse Park-transformation has been adopted to convert $i_{Ld\,(dc)}$ back to i_{1Labc}.

$$\begin{bmatrix} i_{1La} \\ i_{1Lb} \\ i_{1Lc} \end{bmatrix} = \begin{bmatrix} \sin(\omega t) \\ \sin(\omega t - \frac{2\pi}{3}) \\ \sin(\omega t + \frac{2\pi}{3}) \end{bmatrix} \left[i_{Ld(dc)} \right] \quad (16)$$

The sinusoidal reference current i_{Sref} is obtained as

$$i_{Sref} = i_{1Labc} + i_{dc} \quad (17)$$

4. Simulation outcomes with analysis

The three-phase voltage source inverter-based DSTATCOM have been implemented in MATLAB / Simulink to carry out simulation studies. The DSTATCOM topology consists of two categories of diode loads. The first diode load consists parallel connected resistor (of 80 Ω) and capacitor (of 1200 μF). The second diode load consists series connected resistor (of 60 Ω) and inductor (of 50 mH).

Table 1 - Proposed parameters for DSTATCOM

Parameter	Values
Three-phase Supply	$V_{L\text{-}L}$ (rms) =400 V, f = 50 Hz R_s= 1 Ω, L_s= 2mH
Three-phase Unbalanced R-L load	R-L_A= 22 Ω,20mH R-L_B= 35Ω,60mH R-L_C= 70Ω,120mH
Three phase diode (R-L/RC type) load	R-L_{diode}= 60Ω,50mH RC_{diode}= 80Ω,1200 μF
VSI switching device and no.of Leg	IGBTs/diodes and 6-leg
Switching frequency	10 kHz
Inverter (VSI) parameters	C_{dc} = 4000μF, L_f = 20 mH, R_f= 0.1 Ω

The major aspects of these simulations are to study two different performances of DSTATCOM topology i.e. Supply current harmonic mitigation and Improvement of power factor on supply side under the conventional-SRF, DCC based SRF and ICC based SRF control techniques. The total harmonic distortion (THD) measurements of supply current are compared for conventional-SRF, DCC based SRF and ICC based SRF control techniques for Rectified RC/RL Load. The data applicable on the above simulation works are depicted in Table 1.

A. Performance of DSTATCOM under conventional SRF control with non-linear RC/RL Load

In this section performances of DSTATCOM in conventional SRF control with non-linear RC/RL Load are illustrated. Firstly the performance characteristic of the DSTATCOM system is examined in non-linear RC Load condition. Waveform of load current, compensating current, supply current, PCC voltage and PWM pulses are depicted in Fig. 5 for the case of before and after switching.

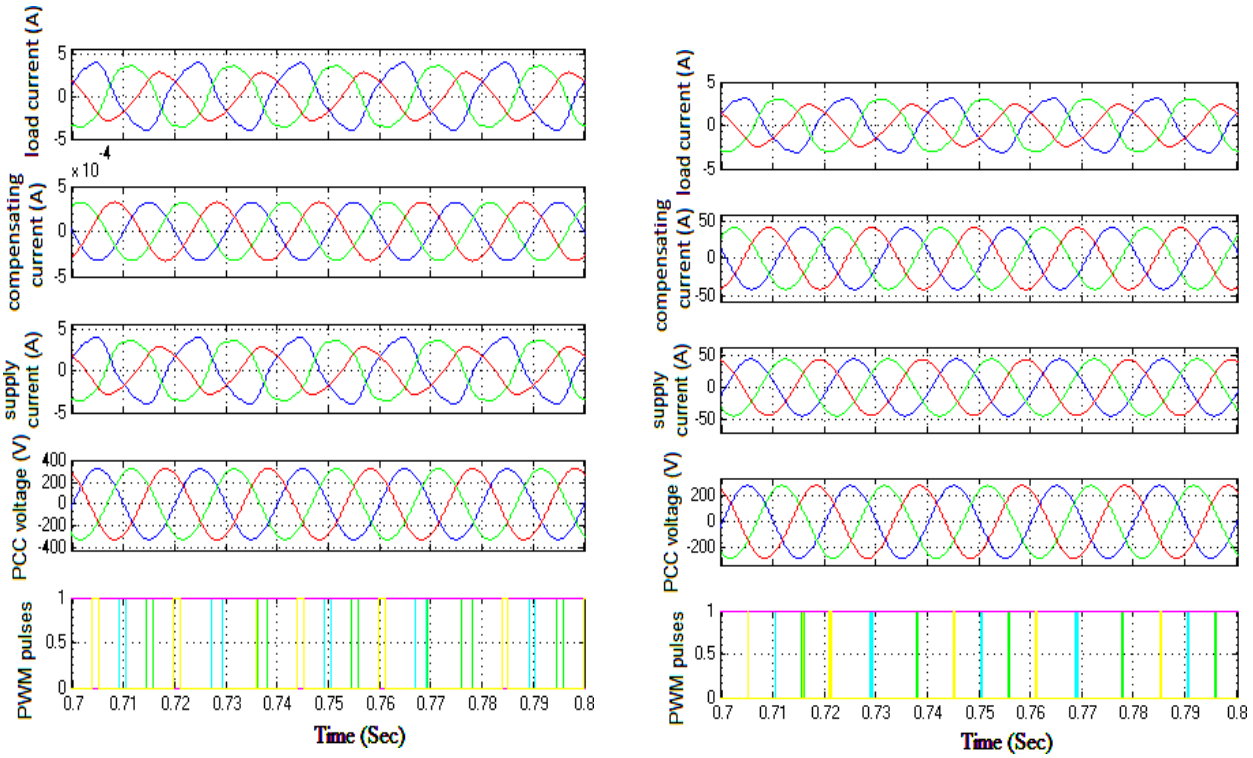

(a) **(b)**

Fig. 5 - Waveforms of DSTATCOM parameters with non-linear RC Load
(a) Before switching (b) After switching
(b)

Before and after switching load current waveform is unchanged. Compensating current waveform is sinusoidal but it indicates approximately zero value on before switching. Source current waveform is becoming balanced and sinusoidal on after switching. Waveform of terminal voltage remains unaltered and is balanced and sinusoidal. PWM waveform appears in the form of pulses. Fig. 6 shows THD reduction of supply current from 12.02% before switching to 3.41% after switching.

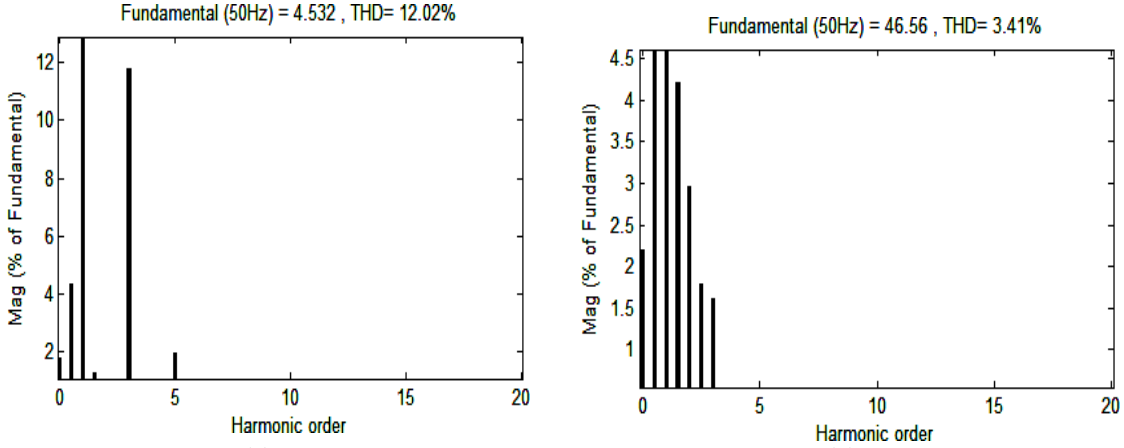

(a) **(b)**

Fig. 6 - Supply current THD for non-linear RC Load
(a) Before switching (b) After switching
(b)

Now the performance of DSTATCOM system is investigated under non-linear RL Load condition. Fig.7 represents various waveforms of current, voltage and PWM pulses of DSTATCOM system.

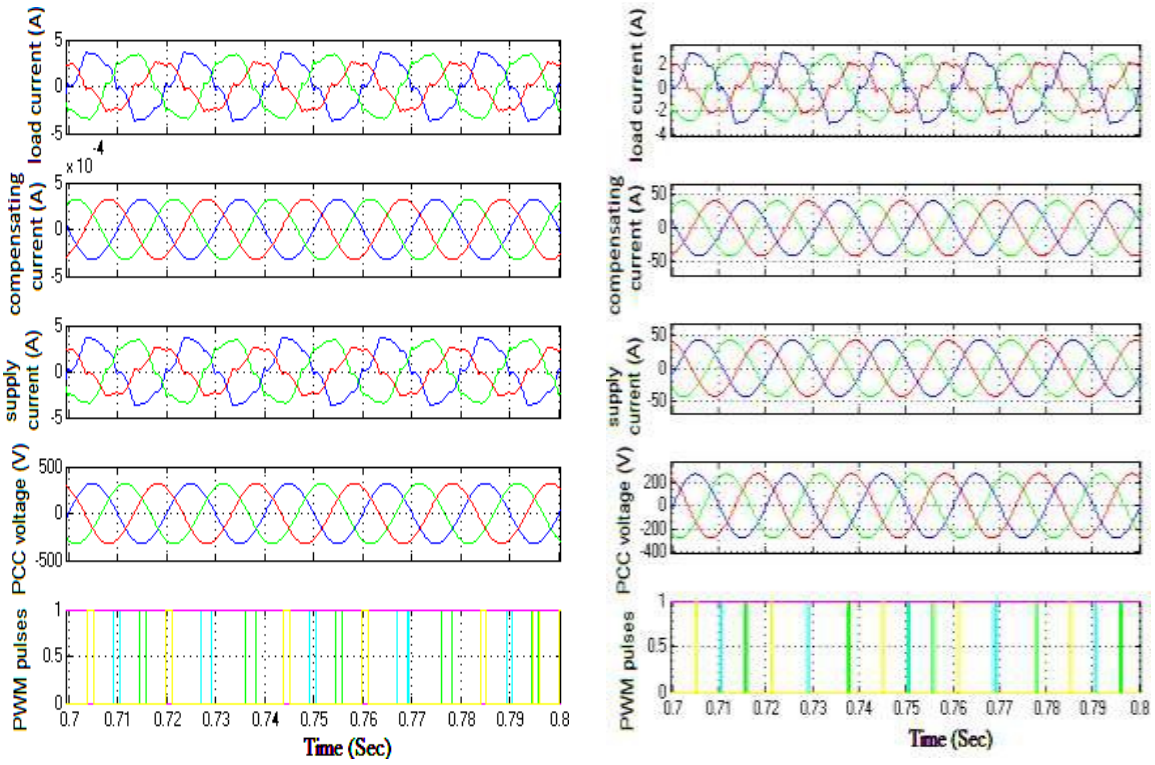

(a) **(b)**

Fig. 7 - Waveforms of DSTATCOM parameters with non-linear RL Load
(a) Before switching (b) After switching

The load current waveform before and after switching is similar but unbalanced and non-sinusoidal. Before switching, compensating current is approximately zero and increased after switching. After switching, non-sinusoidal source current waveform becomes sinusoidal. For both the cases i.e. before and after switching, waveform of terminal voltage remains balanced and sinusoidal in nature. PWM waveform appears in the form of pulse train. Fig. 8 indicates harmonic distortion of source current which is decreased from 13.18% before switching to 3.32% after switching.

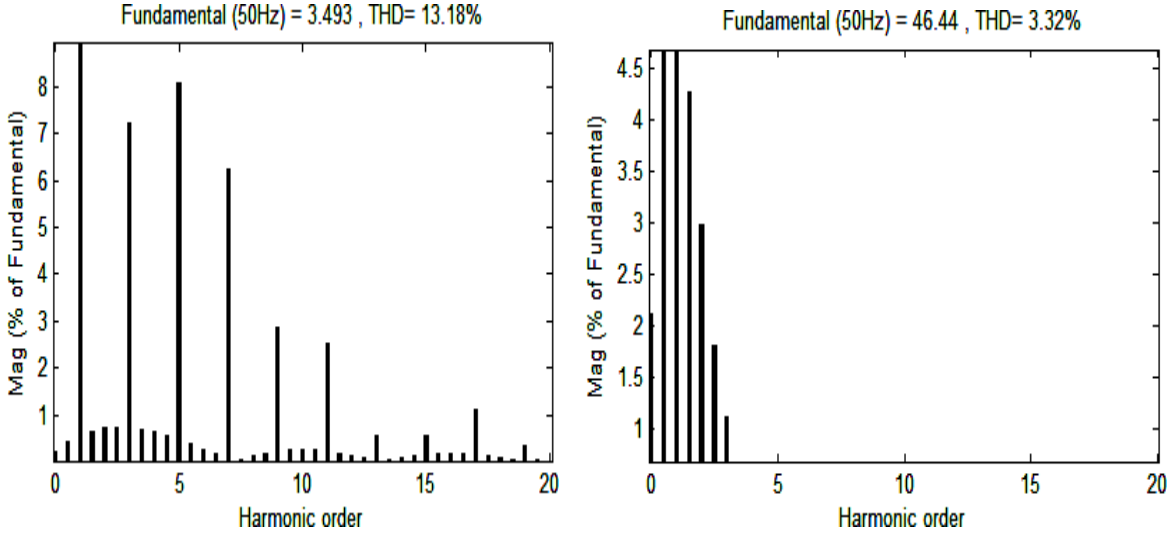

(a) **(b)**

Fig. 8 - Supply current THD for non-linear RL Load
(a) Before switching (b) After switching

B. Performance of DSTATCOM under DCC based SRF control with non-linear RC/RL Load

Fig. 9 represents various waveforms of DSTATCOM system under non-linear RC load condition. The testing parameters are load current, compensating current, supply current, PCC voltage and PWM pulses. In case of before switching, there is a similarity in load current and source current waveforms which are unbalanced and non-sinusoidal in nature. No compensation occurs i.e. compensating current has zero value. Terminal voltage is sinusoidal. After switching, load current waveform is unbalanced and distorted. The sinusoidal waveshape occurs at compensating current, supply current and PCC voltage parameters. It has been found that supply current and PCC voltage are in one phase which represents power factor improvement on the source side. The THD representation of supply current is indicated at Fig.10 where THD value is reduced from 12.02% to 3.18%.

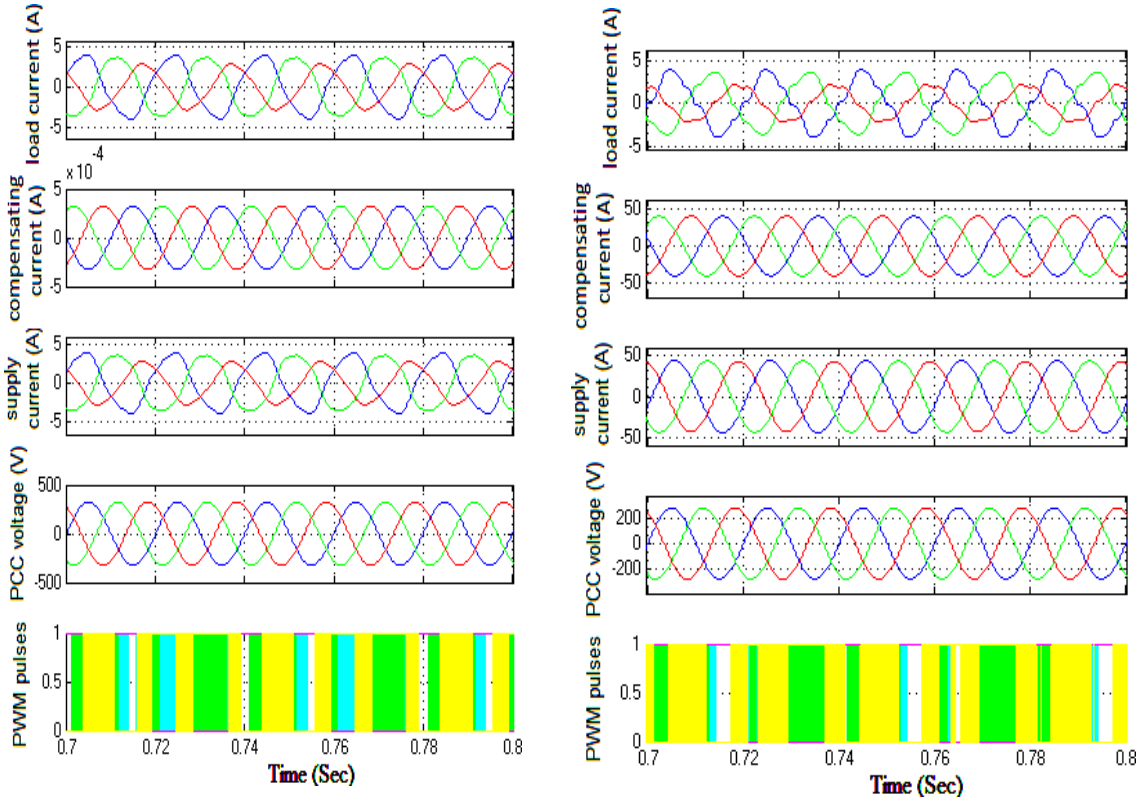

(a) (b)

Fig. 9 - Waveforms of DSTATCOM parameters with non-linear RC Load
(a) Before switching (b) After switching

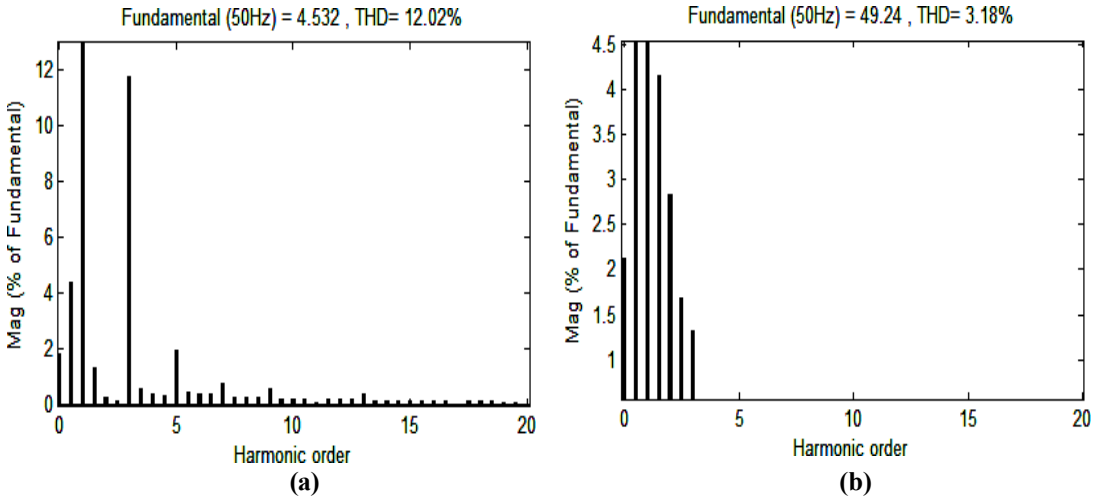

(a) (b)

Fig. 10 - Supply current THD for non-linear RC Load
(a) Before switching (b) After switching

Now the DSTATCOM performance has been tested under non-linear RL load condition as in Fig. 11. Fig. 11 indicates various current, voltage and PWM waveforms in before switching and after switching. For before switching, load current and source current waveform is similar, unbalanced and non- sinusoidal nature. The magnitude of compensating current is approximately zero value. Terminal voltage is pure sinusoidal. After switching, load current waveform is sinusoidal but unbalanced. Compensating current is pure sinusoidal. The source current and terminal voltage waveform are also pure sinusoidal and both are in one phase which represents unity power factor.

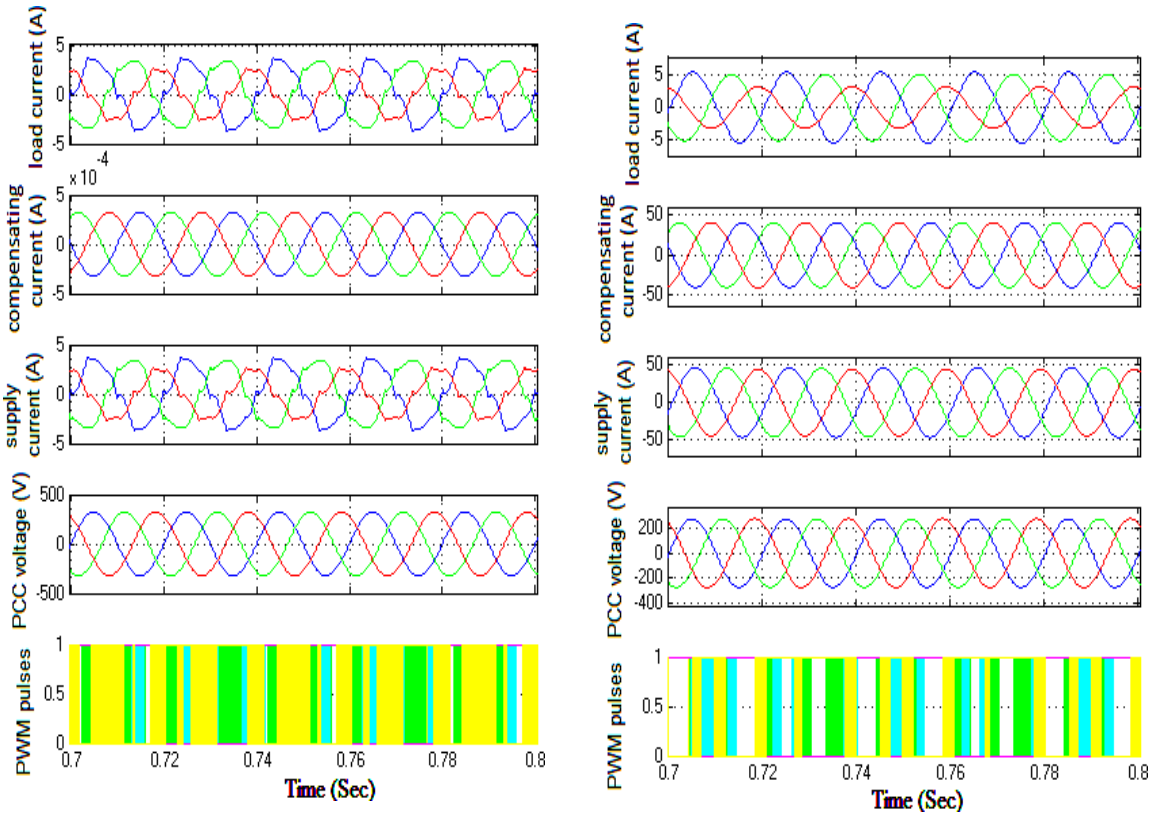

Fig. 11 - Waveforms of DSTATCOM parameters with non-linear RL Load
(a) Before switching (b) After switching

Fig. 12 indicates THD of source current on before and after switching which reduces from 13.18% to 3.01%.

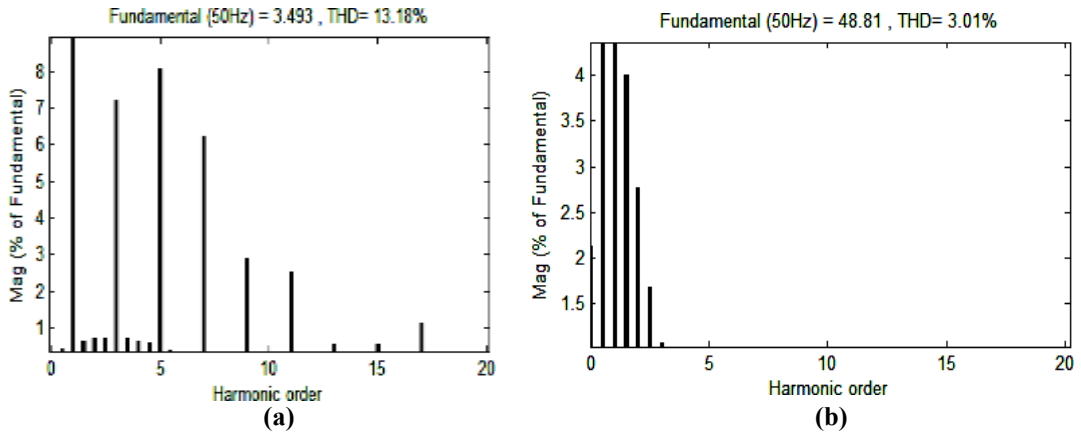

Fig. 12 - Supply current THD for non-linear RL Load
(a) Before switching (b) After switching

C. Performance of DSTATCOM under ICC based SRF control with non-linear RC/RL Load

In this section, the voltage and current characteristic of the DSTATCOM systems in terms of harmonic compensation in Supply current and power factor improvement is illustrated. Firstly the performance characteristic of the DSTATCOM system is tested under non-linear RC Load condition. Fig. 13 depicts voltage, current and PWM waveform for DSTATCOM in before switching and after switching condition.

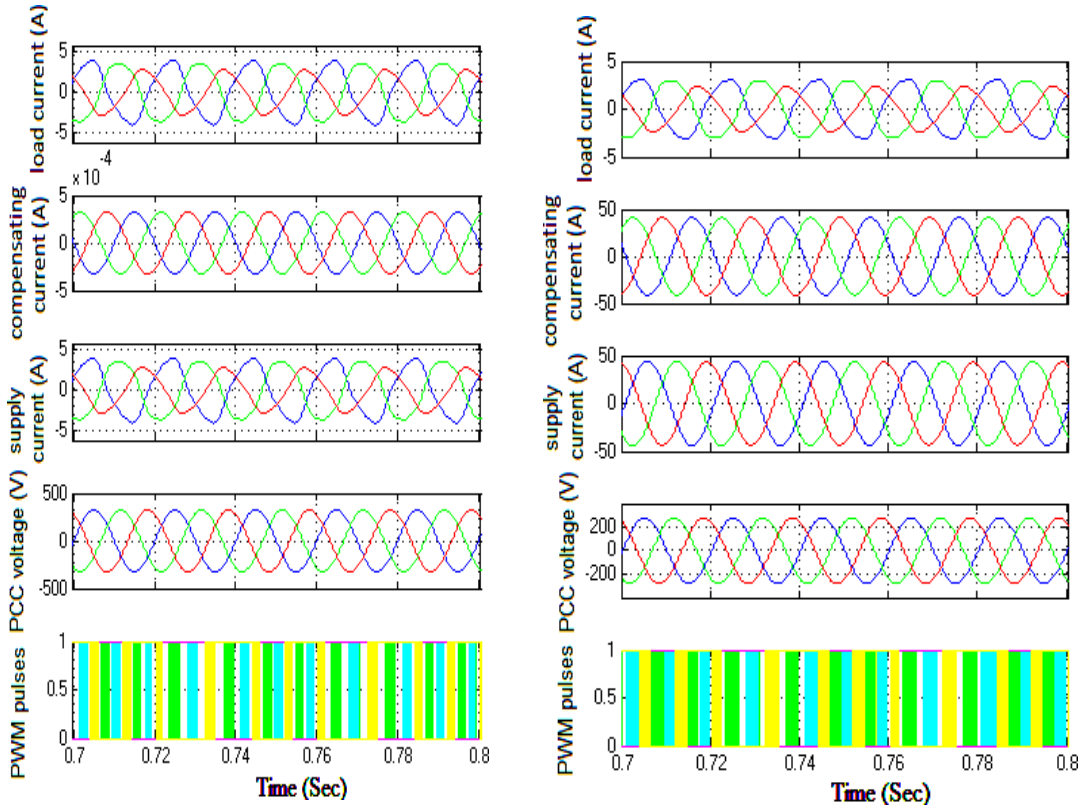

(a) **(b)**

Fig. 13 - Waveforms of DSTATCOM parameters with non-linear RC Load
(a) Before switching (b) After switching

Before switching, there is similarity in waveform of load current and supply current which is non-sinusoidal and distorted. As always, compensating current is zero. Pure sinusoidal voltage waveform occurs at PCC point. After switching, distorted current waveform occurs at load side due to nonlinear load. The compensating current is full sinusoidal wave. However, the magnitude of source current and PCC voltage are different but in-phase which represents power factor improvement on the supply side. The THD of source current is represented in Fig. 14 where THD reduction is achieved from 12.02% (Before switching) to 0.76% (After switching).

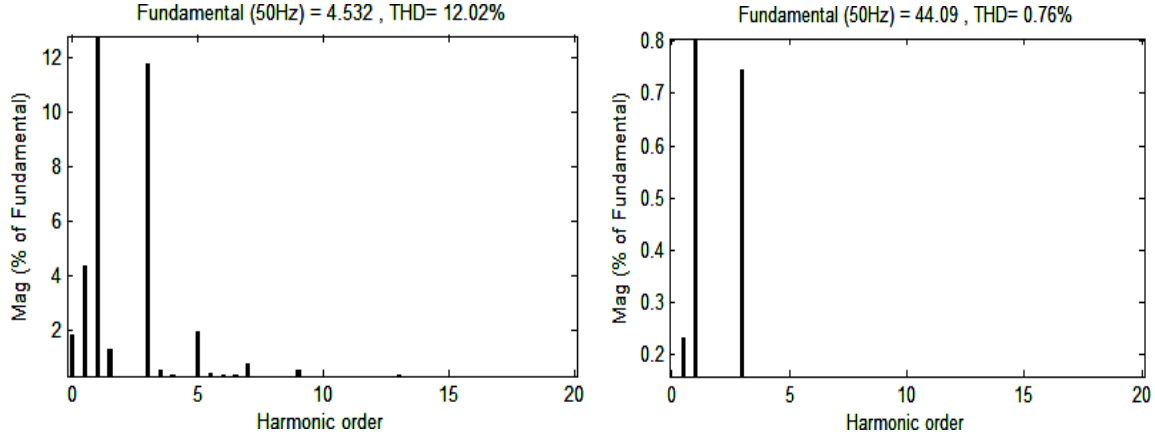

(a) **(b)**

Fig. 14 - Supply current THD for non-linear RC Load
(a) Before switching (b) After switching

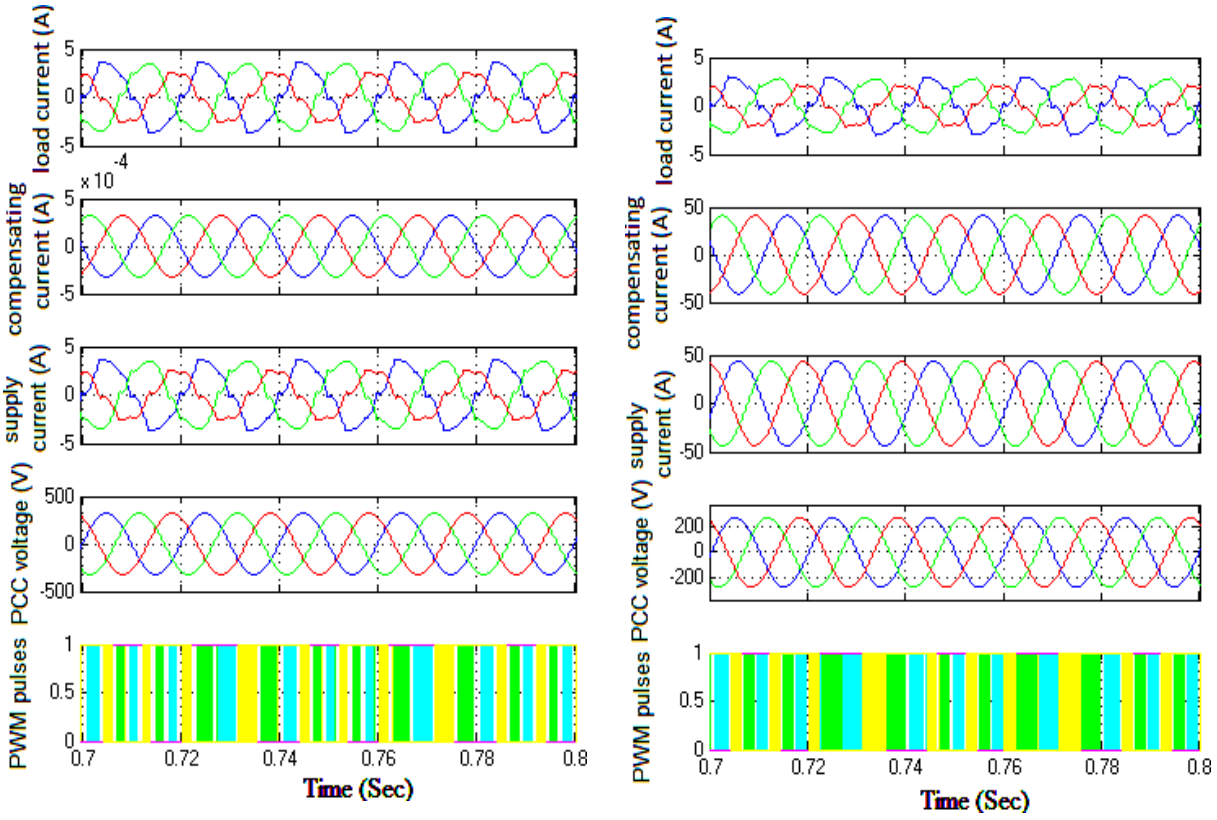

(a) **(b)**

Fig. 15 - Waveforms of DSTATCOM parameters with non-linear RL Load
(a) Before switching (b) After switching

Now the performance characteristic of the DSTATCOM is examined under non-linear RL Load as in Fig. 15. Before switching, Due to unbalanced and diode load, the waveform of load current and supply current are different magnitude at each phase and distorted wave. As usual, no compensation occurs before switching i.e. compensating current is zero. PCC voltage waveform at the coupling point is sinusoidal. After switching, the waveform of load current is non-sinusoidal and unbalanced but supply current waveform becomes pure sinusoidal and in-phase with the terminal voltage which is also sinusoidal nature. PWM pulses appear before and after switching.

The THD spectrum of supply current is represented in Fig. 16 which is decreased from 13.18% (before switching) to 0.74% (after switching).

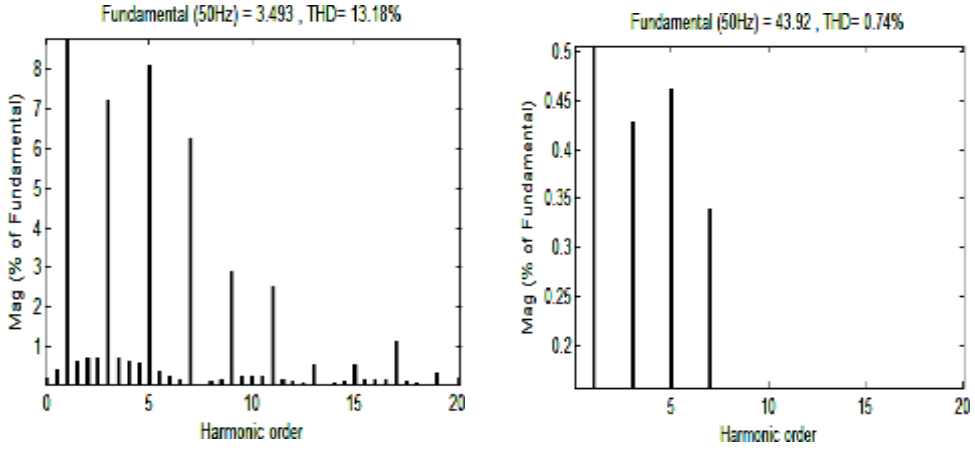

(a) **(b)**

Fig. 16 - Supply current THD for non-linear RL Load
(a) Before switching (b) After switching

Table 2 summarizes THD of supply current of Conventional SRF, DCC based SRF and ICC based SRF DSTATCOM system having Rectified RC/RL Load for the case of before switching and after switching. Fig. 17 indicates its Chartable representation.

Table 2 - %THD of supply current for DSTATCOM in various SRF

SRF Control Strategies	Rectified RC Load		Rectified RL Load	
	Before Switching (%)	After Switching (%)	Before Switching (%)	After Switching (%)
Conventional SRF	12.02	3.41	13.18	3.32
DCC based SRF	12.02	3.18	13.18	3.01
ICC based SRF	12.02	0.76	13.18	0.74

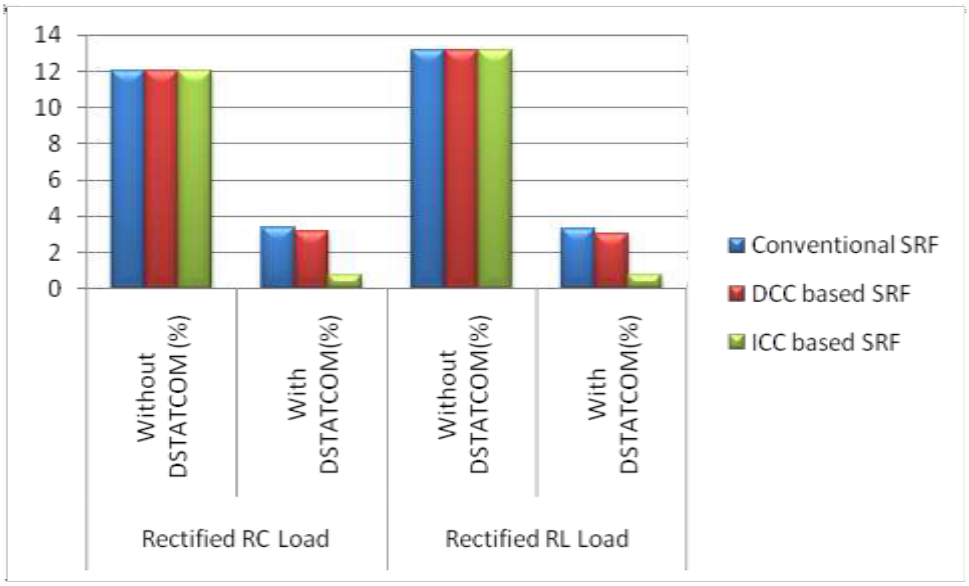

Fig. 17- Chartable form of supply current THD

5. Conclusion

A comprehensive analysis of 3P4W DSTATCOM system is conducted to evaluate the power quality performance in the sense of current harmonic mitigation and power factor improvement. Various SRF algorithms such as Conventional SRF, DCC based SRF and ICC based SRF have been employed in 3P4W DSTATCOM system to achieve power quality improvement task. Additionally, a relative performance assessment of the above SRF algorithms is also accomplished to validate the improvements attained by the proposed ICC based SRF technique. The MATLAB/Simulation based implementation of 3P4W DSTATCOM system demonstrates that the proposed ICC based SRF is the only technique which can be utilized effectively to mitigate the supply current harmonics for all types of nonlinear load and also capable to maintain unity power factor on the source side. The deducted THD value for all SRF algorithms mention in table 2 successfully fulfills the criteria of IEEE-519 harmonic standard.

Acknowledgements

This work has been financially supported by the NIT Sikkim, MHRD, Govt. of India, New Delhi.

References

[1] Kusko, A. & Thompson, M. T. (2007). Power quality in electrical systems. McGraw-Hill, New York.
[2] Mishra, S. & Ray, P. K. (2016). Power quality improvement using photovoltaic fed DSTATCOM based on JAYA optimization. IEEE Trans. Sustain. Energy, 7, 1672-1680.
[3] Heydt, G. T. (1994). Electric Power Quality. 2nd ed., Stars in a Circle, USA.
[4] Miller, T. J. E. (1982). Reactive Power Control in Electric Systems. Wiley, USA.

[5] Arrilaga, J., Wattson, N. R. & Chen, S. (2000). Power System Quality Assessment. Wiley, USA.
[6] Sankaran, C. (2001). Power Quality, CRC Press, USA.
[7] Ghosh, A. & Ledwich, G. (2002). Power quality enhancement using custom power devices, Kluwer Academic Publishers, London.
[8] Dugan, R. C., McGranaghan, M. F. & Beaty, H. W. (2006). Electric Power Systems Quality, 2nd ed., McGraw Hill, USA.
[9] Moreno-Munoz, A. (2007). Power Quality: Mitigation Technologies in a Distributed Environment. Springer-Verlag, Germany.
[10] Singh, B., Chandra, A. & Al-Haddad, K. (2015). Power quality: problems and mitigation techniques, Wiley, U.K.
[11] Latran, M. B., Teke, A. & Yoldas, Y. (2015). Mitigation of power quality problems using distribution static synchronous compensator: a comprehensive review. IET Power Electron. 8, 1312-1328.
[12] George, V. & Mishra, M. K. (2010). DSTATCOM topologies for three-phase high power Applications. Int. J. Power Electron., 2, 107-124.
[13] Kumar, Pradeep, Kumar, Niranjan & Akella, A.K. (2013). Modeling and Simulation of Different System Topologies for DSTATCOM. AASRI Procedia, 5, 249 - 261.
[14] Kumar, Pradeep (2017). Comparative Power Quality analysis of Conventional and Modified DSTATCOM Topology. International Journal on Electrical Engineering and Informatics, 9, 786-799.
[15] Kumar, Pradeep, Kumar, Niranjan & Akella, A.K. (2016). Comparative analysis of voltage and current source inverter based DSTATCOM. Turkish Journal of Electrical Engineering & Computer sciences, 24, 3838 - 3851.
[16] Monfared, M., Golestan, S. & Guerrero, J. M. (2013). A new synchronous reference frame-based method for single-phase shunt active power filters. Journal of Power Electronics, 13, 692-700.
[17] Dey, P. & Mekhilef, S. (2014). Synchronous reference frame based control technique for shunt hybrid active power filter under non-ideal voltage. in IEEE Innovative Smart Grid Technologies - Asia (ISGT Asia), 481-486.
[18] Padiyar, K. R. (2007). FACTS Controllers in Transmission and Distribution. New Age International, New Delhi, India.
[19] Kumar, Pradeep, Kumar, Niranjan & Akella, A.K. (2014). A Simulation Based Case Study for Control of DSTATCOM. ISA Transactions, 53,767-775.
[20] Akagi, H., Watanabe, E.H. & Aredes, M. (2007). Instantaneous Power Theory and Applications to Power Conditioning, Wiley, Hoboken, NJ.
[21] Syed, M. K. & Ram, B. S. (2008). Instantaneous power theory based active power filter: a matlab/simulink approach. Journal of Theoretical & Applied Information Technology, 4, 536-541.
[22] Forghani, M. & Afsharnia, S. (2007). Online wavelet transform-based control strategy for UPQC control system. IEEE Trans. Power Del., 22, 481-491.
[23] Radzi, M. A. M. & Rahim, N. A.(2009). Neural network and bandless hysteresis approach to control switched capacitor active power filter for reduction of harmonics. IEEE Trans. Ind. Electron., 56, 1477-1484.
[24] Singh, B., Verma, V. & Solanki, J. (2007). Neural network-based selective compensation of current quality problems in distribution system. IEEE Trans. Ind. Electron., 54, 53-60.
[25] Baggini, Angelo (2008). Hand Book of power quality, John Wiley & Sons Ltd, England.
[26] Plantive E., Courtois C., Poirrier J. P. & Javerzac J. L. (2000). Application of a 20MVA STATCOM for voltage balancing and power active filtering of a 25 kV AC single-phase railway substation connected to the 90 kV grid in France. CIGRE 13/14/36-12.
[27] Marks, J. H. & Green, T. C. (2002). Predictive transient-following control of shunt and series active power filters. IEEE Trans. Power Electron., 17, 574-584.
[28] Diwan, S. P., Inamdar, H. P. & Vaidya, A. P. (2011). Simulation studies of shunt passive harmonic filters: six pulse rectifier load power factor improvement and harmonic control. ACEEE International Journal on Electrical and Power Engineering, 2, pp. 1-6.
[29] Larsson T. & Ekstrom A. (1997). A PWM-operated voltage source converter for flicker mitigation. European Power Electronics Conference, 3, 1016-1020.
[30] Hoon, Yap, Radzi, Mohd Amran Mohd, Hassan, Mohd Khair, Mailah, Nashiren Farzilah & Wahab, Noor Izzri Abdul (2016). A Simplified Synchronous Reference Frame for Indirect Current Controlled Three-level Inverter-based Shunt Active Power Filters. Journal of Power Electronics, 16, 1964-1980.
[31] Chen, Donghua & Xie, Shaojun (2004). Review of the control strategies applied to active power filters. IEEE International Conference on Electric Utility Deregulation, Restructuring and Power Technologies, 666-670.
[32] Montero, Maria Isabel Milanes, Cadaval, Enrique Romero & Gonzalez, Fermin Barrero (2007). Comparison of Control Strategies for Shunt Active Power Filters in Three-Phase Four-Wire Systems. IEEE Trans on Power Electronics, 22, 299-236.
[33] Lee,Tzung-Lin & Hu, Shang-Hung (2011). Discrete Frequency-Tuning Active Filter to Suppress Harmonic Resonances of Closed-Loop Distribution Power Systems. IEEE Trans on Power Electronics, 26, 137-148.

[34] Pigazo, Alberto, Moreno, Victor M. & Estebanez, Emilio J. (2009). A Recursive Park Transformation to Improve the Performance of Synchronous Reference Frame Controllers in Shunt Active Power Filters. IEEE Trans on Power Electronics, 24, 2065-2075.
[35] Karuppanan, P & Mahapatra, Kamala kanta (2010). A Novel SRF Based Cascaded Multilevel Active Filter for Power Line Conditioners. IEEE INDICON,1-4.
[36] Pouresmaeil, Edris, Montesinos-Miracle, Daniel, Gomis-Bellmunt, Oriol & Bergas-Jane, Joan (2010). A multi-objective control strategy for grid connection of DG (distributed generation) resources. Energy, 35, 5022-5030.